ELSEVIER

Journal of Power Sources 89 (2000) 206–218

JOURNAL OF POWER SOURCES

www.elsevier.com/locate/jpowsour

Review of selected electrode–solution interactions which determine the performance of Li and Li ion batteries

Doron Aurbach *

Department of Chemistry, Bar-Ilan University, Ramat-Gan 52900, Israel

Received 16 September 1999; accepted 1 February 2000

Abstract

We report herein on several phenomenological electrode–solution interactions which determine the performance of lithium and lithium ion batteries. This review is based on extensive studies of the behavior of Li, lithiated carbons and lithiated transition metal oxide electrodes in a wide variety of non-aqueous electrolyte solutions. These studies included spectroscopic measurements (FTIR, XPS, EDAX), morphological and structural analysis (XRD, SEM, AFM) in conjunction with impedance spectroscopy, EQCM and standard electrochemical techniques. It appears that the performance of both Li, Li–C anodes and Li_xMO_y cathodes depends on their surface chemistry in solutions. We address complicated surface film formation on these electrodes, which either contribute to electrode stabilization or to capacity fading due to an increase in the electrodes' impedance. Several common classical phenomena occurring in these systems are reviewed and discussed.

Keywords: Electrode–solution interactions; Lithium; Lithium ion batteries

1. Introduction

There is an increasing worldwide demand for high energy density batteries. The current major vehicles' lead acid ($Pb–PbO_2$) and NiCd (Cd–NiOOH) batteries prove 40 W h/kg (1–2 V). It is possible to increase the energy density of practical batteries up to 120–160 W h/kg. This target can be achieved using active metal anodes (very low potential) and a high voltage red-ox cathode ($V > 3$ V in the M/M^{+z} scale). The first choice of an anode for such batteries is, naturally, lithium.

The cathodes can be different red-ox couples, including positively doped, electronically conducting polymers [1] and polysulfides [2]. However, so far the best choice for cathodic reactions for Li batteries are Li intercalation reactions into transition metal oxides and sulfides [3].

$$Li^+ + e^- + Li_xMO_y \rightarrow Li_{1+x}MO_y \quad (1)$$

$$Li^+ + e^- + Li_xMS_y \rightarrow Li_{1+x}MS_y \quad (2)$$

Examples are $LiMnO_2$ (orthorhombic, 3 V), VO_x (3 V), $LiMn_2O_4$ (spinel, 4 V) $LiNiO_2$, $LiCoO_2$ (4 V), etc.

The major demand for the electrolyte systems for these batteries is electrochemical windows around 4–5 V. The options are polar aprotic solvents with Li salts operating at $-40°C < T < 60°C$, polymers such as PEO and its derivatives (e.g. branched polymeric chains) + Li salts operating at $T > 60°C$, and polymers + solvents + Li salts (gel systems), operating at a wide temperature window (similar, perhaps, to that of liquid systems). Rechargeable Li metal batteries became a commercial reality [4]. However, Li metal based batteries may have some drawbacks, which include limited cyclability of the Li electrodes (dendritic deposition, shorting, the electrolyte solution disappears due to reactions with reactive lithium). There are also potential safety problems in their use due to the occurrence of thermal runaway in abuse cases.

An alternative to Li metal batteries is the rocking chair'' concept, in which a **low** potential Li insertion anode is used with a **high** potential Li insertion cathode. These battery systems function according to the following equation [5]:

$$Li_xC_6 + Li_yMO_z \Leftrightarrow C_6 + Li_{y+x}MO_z, \quad (3)$$

where $x \approx 1$ = graphite, $x < 1$ = soft carbon, $x > 1$ = hard, disordered carbon, M = Mn, Ni, Co, V, etc.

* Tel.: +972-3-535-1250.
E-mail address: aurbach@gefen.cc.biu.ac.il (D. Aurbach).

0378-7753/00/$ - see front matter
PII: S0378-7753(00)00431-6

These battery systems became a commercial reality, and many of them are available in a variety of configurations, size and capacity [6–8]. However, despite of the fact that they are a commercial reality, there is still a long way to go in this field:

(a) R&D of non-reactive polymeric systems for these batteries operating at room temperature.
(b) 5 V cathodes and 3 V cathodes, which are stable and of high capacity.
(c) **Reproducible** engineering of high capacity (Li_xC_6), $x > 1$) carbon anodes.

There is also a real chance for R&D of Mg and Al rechargeable non-aqueous batteries based on metal insertion cathodes (and these active metal anodes).

In reviewing the recent literature in electrochemistry and material science, one notices how vital is the research related to high energy density, rechargeable batteries, especially those which are based on metal insertion reactions into host materials. Below, we list a few examples of new directions in the research related to these systems.

- Synthesis of cathodes (e.g. the work of Armstrong et al. [9], Kawai et al. [10] and Fey et al. [11]).
- New and reproducible synthetic routes for hard carbons, which include surface and 3D engineering (e.g. the work of Buiel et al. [12]).
- The study of capacity fading mechanisms (e.g. the extensive work of Amatucci et al. [13]).
- Theoretical studies in which phase diagrams and voltage profiles for Li_xMO_y compounds are calculated (e.g. Ceder et al.'s [14] and Ohzuku's [15] work).
- Better 3D and morphological analysis of exotic anode materials. Examples are the use of neutron diffraction by Teslic et al. [16], SPM by Inaba et al. [17] and solid state NMR by Menachem et al. [18]
- Development of new experimental tools. Solid state NMR, EXAFS, XANES, ARC-DSC, Mössbauer spectroscopy, in situ Raman, SIM-TOF, etc.
- New synthetic routes for cathode materials, especially in thin films. Example: Pulse laser deposition (PLD) by Ginley et al. [19]
- Development of new solutions by companies such as Merck.
- Development of nonreactive, low temperature conducting polymers [20].
- R&D of Mg and Al rechargeable batteries (e.g. the work of Novak et al. [21] on Mg insertion electrodes).

Another important direction in the research on active metal and Li insertion electrodes for high energy density batteries relates to their surface chemistry. During the past 15 years, we studied extensively the correlation amongst the surface chemistry, 3D structure, morphology, impedance and electrochemical behavior of Li, lithiated carbon, Mg and Li_xMO_y (M = Ni, Co, Mn, V, etc.) electrodes in a large variety of non-aqueous (polar aprotic) electrolyte solutions [22–24].

Information on the surface chemistry of these systems was obtained from FTIR, XPS and EDAX measurements, morphological aspects were studied by SEM, AFM and STM, 3D structure was measured by in situ and ex situ XRD, while characterization of the electrochemical behavior of these systems was carried out by a variety of techniques, including impedance spectroscopy (EIS), galvanostatic and potentiostatic intermittent titrations (GITT, PITT), variable scan rates, cyclic voltammetry, chronopotentiometry, chronoamperometry and electrochemical quartz crystal microbalance (EQCM).

This paper reviews several phenomena that are common to anodes and cathodes in high energy density batteries, and relates to electrode–solution interactions. The phe-

Table 1
References for previous work on the various methods of electrode characterizations using spectroscopic and electrochemical techniques

No	Subject	Refs.
1	Li electrode preparation in solutions	[25]
2	Carbon electrode preparations	[26,27]
3	Mg electrode preparation in solutions	[28]
4	Preparation of cathodes (Li_xMO_y, M = Ni, Co, Mn, etc.)	[29]
5	FTIR spectroscopy of Li electrodes	[25,30]
6	In situ FTIR spectroscopy of active electrodes	[31]
7	FTIR spectroscopy of carbon and Li_xMO_y electrodes	[24,29]
8	Impedance spectroscopy of Li electrodes	[32,33]
9	Electroanalytical studies of composite electrodes (Li–C, Li_xMO_y, etc.)	[26,27,29]
10	Structural studies of Li–C and Li_xMO_y electrodes by in situ XRD	[34,35]
11	Studies of active electrodes in polar aprotic systems by AFM	[36]
12	Studies of active electrodes by EQCM	[37]
13	Studies of nonactive electrodes polarized to low potentials in non-aqueous solutions by spectroscopic and electroanalytical tools (EIS, FTIR, CV, etc.)	[38]
14	Studies related to practical Li batteries (e.g. AA cells)	[4,39,40]
15	XPS measurements of Li and Li–C electrodes	[30,41]

nomena reported here are connected to stabilization and failure mechanisms of these systems.

2. Experimental

We used carbonaceous materials from Timcal and Superior Graphite, and cathode materials and ready to use, highly pure electrolyte solutions from Merck. All the measurements and preparations for the various spectroscopic studies were conducted under highly pure atmosphere in glove boxes equipped with H_2O and O_2 removal systems (from VAC or M. Brown) The various spectroscopic, morphological, structure and electrochemical measurements of Li, Mg, Li–C and Li_xMO_y electrodes were described in previous publications. The following table provides appropriate references to the experimental work which led to the results described in this paper.

It should be noted that the list in Table 1 refers to papers in which the experimental work is described in detail.

3. Results and discussion

3.1. Stabilization and failure of lithium anodes

A prerequisite for the research on the stabilization and failure mechanisms of Li electrodes was an extensive study of the surface chemistry of lithium electrodes in a variety of electrolyte solutions. The major tools for these studies were surface sensitive FTIR spectroscopy, EDAX and XPS. We also tried other tools such as AES and Raman spectroscopy, although the most useful source of information was a combination of FTIR spectroscopy and XPS. The former technique is non-destructive and provided identification of the functional groups and types of bonds on the Li surfaces. The latter technique may provide similar information, but it may be destructive to the Li surface [42]. By choosing appropriate working conditions it was possible to minimize the detrimental effect of the X-ray beam on the surface films on lithium [41,42]. In general, the major solvent reduction products that precipitate on lithium electrodes in ethers, esters and alkyl carbonate solutions (which are the most important solvents for Li batteries) were ROLi, RCOOLi and $ROCO_2Li$ species, respectively [22–24]). By comparative experiments which included solvent reduction by electrolysis, Li/Hg amalgam and Li powder [43], it was possible to identify specific surface components formed on Li electrodes, such as $(CH_2OCO_2Li)_2$ and $CH_3CH(OCO_2Li)CH_2OCO_2Li$ formed by reduction of ethylene and propylene carbonates [22–24] (EC and PC, respectively), CH_3OLi and CH_3OCO_2Li formed by reduction of dimethyl carbonate, HCOOLi formed by reduction of methyl formate [44], etc. XPS revealed that Li salt with perfluorinated anions of the MF_y^- type (M = As, P, B) are reduced on Li to surface LiF and species of the Li_xMF_y type. XPS also revealed that the surface films formed on lithium in all solutions (ether, ester, alkyl carbonates) contain species with Li–C bonds. Hence, taking the commonly used electrolyte system, EC-DMC/$LiPF_6$ solutions, we can outline the following reaction scheme for the surface film formation on Li in this system, based on the above studies [30,42,43].

$$2EC + 2e^- + 2Li^+ \rightarrow (CH_2OCO_2Li)_2\downarrow + CH_2{=}CH_2\uparrow. \quad (4)$$

$$EC + 2e^- + 2Li^+ \rightarrow LiCH_2CH_2OCO_2Li\downarrow. \quad (5)$$

$$DMC + e^- + Li^+ \rightarrow CH_3\cdot + CH_3OCO_2Li\downarrow \text{ and/or } CH_3OLi\downarrow + CH_3OCO\cdot. \quad (6)$$

$$\text{Trace}\, H_2O + e^- + Li^+ \rightarrow LiOH\downarrow + 1/2H_2\uparrow. \quad (7)$$

$$LiOH + e^- + Li^+ \rightarrow Li_2O\downarrow + 1/2H_2\uparrow. \quad (8)$$

$$H_2O + (CH_2OCO_2Li)_2 \rightarrow Li_2CO_3 + CO_2 + (CH_2OH)_2. \quad (9)$$

$$2CO_2 + 2e^- + 2Li^+ \rightarrow Li_2CO_3\downarrow + CO\uparrow. \quad (10)$$

$$LiPF_6 \rightleftharpoons LiF + PF_5; PF_5 + H_2O \rightarrow 2HF + PF_3O. \quad (11)$$

$$PF_5^- + ne^- + nLi^+ \rightarrow LiF\downarrow + Li_xPF_y\downarrow. \quad (12)$$

$$PF_3O + ne^- + nLi^+ \rightarrow LiF\downarrow + Li_xPOF_y\downarrow. \quad (13)$$

$$HF + (CH_2OCO_2Li)_2\downarrow, Li_2CO_3\downarrow \rightarrow LiF\downarrow + (CH_2COCO_2H)_2, H_2CO_3(\text{sol.}). \quad (14)$$

Note that Eqs. 12–14 do not provide the exact stoichiometry, but rather the basic reactions. In addition, the radical formed in reaction 6 above, may further react with lithium to form surface compounds with Li–C bonds, or can recombine to form gases such as ethane or can disproportionate to form different gases such as H_2, CH_4 and solution species. Recent studies of gaseous products evolving from reactions of EC-DMC mixtures on lithiated carbons correlate to the reaction scheme above and to the attached notes.

XPS provided further important information by depth profiling (sputtering the electrode's surface with argon, followed by element analysis). The surface films formed on Li electrodes in electrolyte solutions have a multilayer structure [41,42,45–47]. Close to the Li surface, the components of the surface films contain mainly species of low oxidation states such as Li_2O, Li_3N, LiX (X = F, Cl, etc.) and lithiated carbon moieties. The outer part of the surface films (solution side) is comprised of species of higher oxidation states, such as $ROCO_2Li$, ROLi, LiOH, Li_xMF_y (M = As, B, P, etc.), $RCOO_2Li$, etc.

AFM, impedance spectroscopy and XPS measurements of Li electrodes in polar aprotic solutions converge to a picture in which the surface films covering lithium electrodes in solutions are comprised of a multilayer inner compact part, several tens to 100-Å thick, and an outer (solution side) porous part [32,33,36,41]. We can present the following scenario for the formation of multilayer films on Li electrodes.

(1) A Li electrode covered with pristine films comes into contact with the solution. The pristine films are usually comprised of Li_2O (inner part) and LiOH, Li_2CO_3 (outer side) [48]. There is a partial dissolution of the pristine film in many solutions [49] and possible nucleophilic reactions of the Li_2O, LiOH species with electrophilic solvent molecules such as esters or alkyl carbonates [50].

(2) Consequently, there is a partial or total replacement of the pristine film by surface species originating from reaction of solution species with the active metal.

(3) Continuous reduction of surface species near the film's Li interface forms a layer of species of low oxidation states, while in the outer part of the surface films there is dynamic precipitation and dissolution of surface species which form a porous structure.

(4) Anodic processes (Li dissolution) accelerate the breakdown of the pristine surface films, thus allowing a more intense reaction of Li with solution species.

(5) When bare Li is exposed to solution (e.g. due to massive deposition which forms fresh Li deposits), there are immediate reactions between Li and solution species in time constants of milliseconds and less [51] which form a first surface layer under non-selective conditions (high reactivity). Further reduction of solution species takes place under more selective conditions via electron transfer through the continuously built up surface layer. This process also leads to a multilayer structure due to the decrease in the driving force of the solution–lithium reactions as the surface films become thicker.

(6) Further changes in the surface film structure take place due to reduction of surface species close to the Li–film interface, as explained above, and possible diffusion of water. This last process is inevitable, as even the purest non-aqueous solutions contain several tens of ppm of water. The surface species formed on Li in the commonly used non-aqueous solutions are highly hygroscopic, and thereby, water from the solution phase penetrates the surface films, hydrates the surface species, thus diffusing towards the active metal. Water reactions take place within the film according to reaction formulae 7 and 9 above [52].

In conclusion, all the scenarios described above lead to a coverage of Li electrodes in multilayer surface films which are comprised mostly of organic or inorganic, relatively small ionic molecules which are, in fact, Li salts. As discussed extensively by Peled [53] (the SEI model), all these Li salts, when deposited as thin surface films, are Li ion conductors. Thereby, applying an electrical field to Li electrodes enables electrochemical Li dissolution and deposition to occur through these surface films. Upon Li

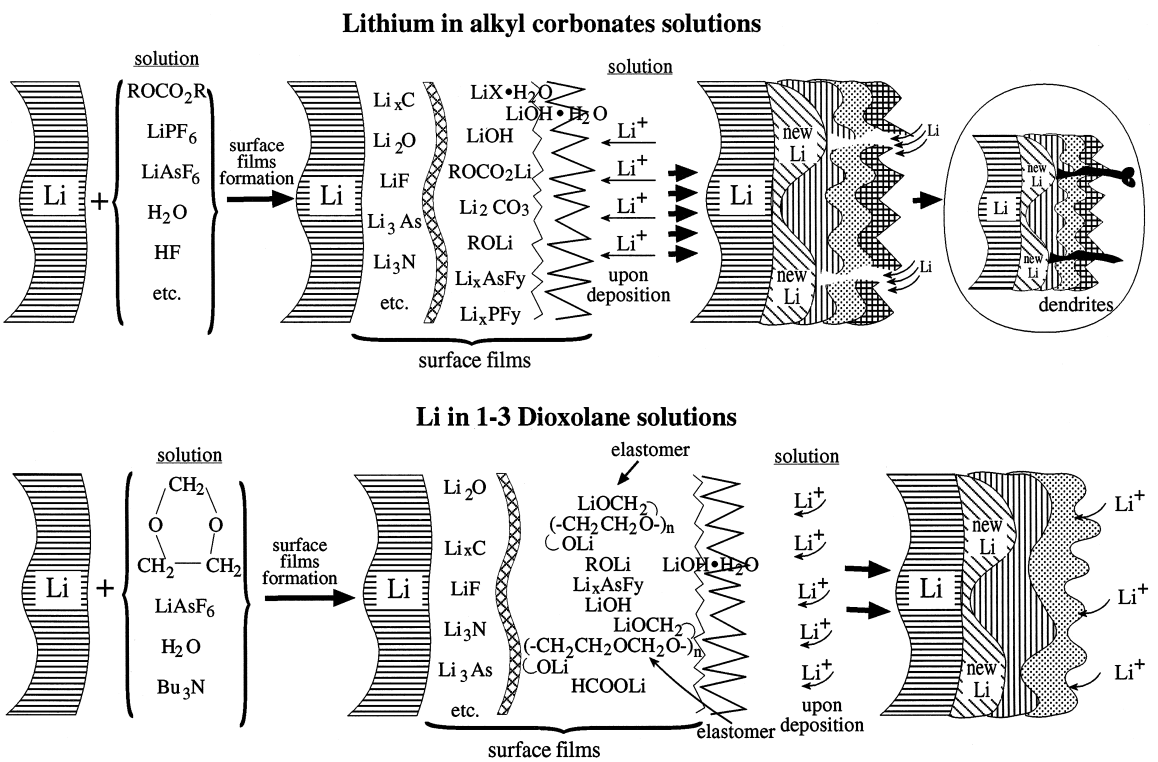

Fig. 1. A schematic illustration of surface film formation on lithium electrodes in alkyl carbonates and in 1-3 dioxolane solutions.

deposition and dissolution, the surface films comprised of ionic species cannot accommodate the morphological change of the Li surface due to these processes, and thus can be broken down, leading to highly non-uniform Li deposition which can form dendrites, as illustrated in Fig. 1, upper part.

This scenario is, in fact, the major failure of Li electrodes as anodes for rechargeable batteries. A breakdown of the surface films due to electrochemical processes of the Li electrodes also leads to further reaction of the bare Li thus formed with solution species. Hence, both Li and solution components are lost upon repeated Li deposition–dissolution process. In addition, the dendrites thus formed due to the non-uniform current distribution as described schematically in Fig. 1 lead to safety problems: shorting, formation of high area reactive lithium, etc. Indeed, cycling efficiency of Li electrodes measured in laboratory tests in all commonly used alkyl carbonates, ester solutions, and in most of the commonly used ethereal solutions, is too low for their use in practical rechargeable Li batteries. One exception is a solution of 1-3 dioxolane (DN), especially when the salt is $LiAsF_6$ [54]. (Stabilization with a base such as tributylamine (TBA) is then required in order to avoid polymerization of the solvent

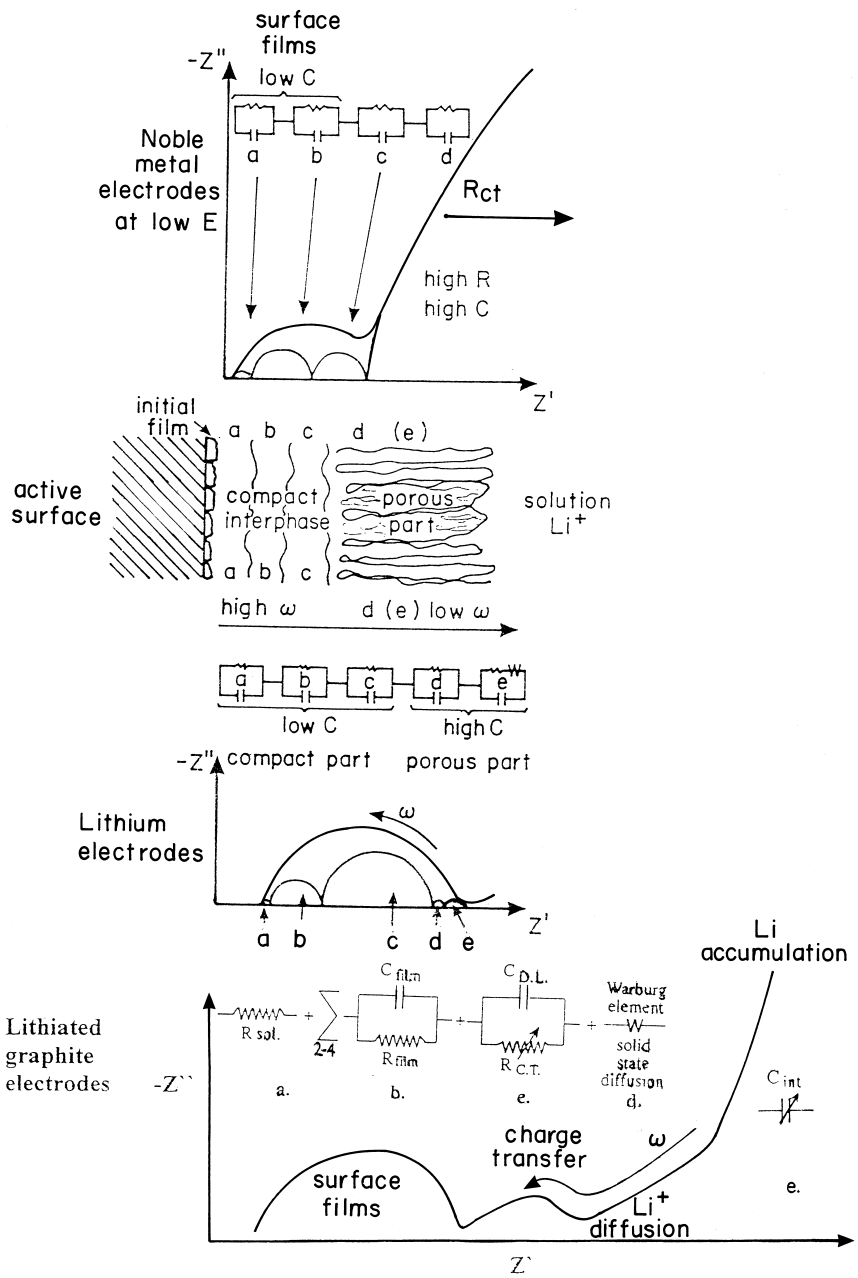

Fig. 2. A schematic illustration of impedance spectra, relevant equivalent circuit analogs, and the structure of the surface films for lithium, lithiated graphite electrodes, and noble metal electrodes polarized to low potentials in Li salt, non-aqueous solutions.

[55]). Li cycling efficiency in DN solutions is very high, and Li deposition morphology in them is very smooth. This allowed the use of these solutions in commercial rechargeable Li batteries [4,39,40].

Understanding the improved performance of Li electrodes in DN solutions is very important as it can lead to the development of improved stabilization mechanisms for Li metal electrodes in practical secondary batteries. The explanation for the improved reversibility of Li electrodes in DN solutions is illustrated in Fig. 1 (lower part). The surface films formed on Li in DN solution contain, in addition to ionic species such as HCOOLi, $CH_3CH_2OCH_2OLi$ (DN reduction products), LiF and Li_xAsF_y (salt reduction products), oligomers of polydioxolane. These are formed by partial polymerization of DN via an anionic mechanism, as already suggested [55], which is possible because DN is a cyclic acetal. The polyDN oligomers are insoluble and adhere to the Li surface because they have alkoxy (OLi) edge groups. Hence, the surface films on lithium in this solvent contain elastomers which make the surface layer much more flexible than the above described fully ionic surface layers formed on Li in other electrolyte solutions. Hence, when Li is deposited or dissolved in these systems, the flexible surface films can better accommodate the volume changes of the active metal, thus providing good passivation to the Li deposits.

As already discussed in detail, SEM [56] and EQCM [37] measurements of Li electrodes cycled in DN solutions were highly in line with the passivation model shown in Fig. 1, which is based on the concept of flexible surface films, and which is probably unique to this system. The exceptionally and surprisingly high Li cycling efficiency obtained in Li-PEO-based batteries at elevated temperatures, as was reported recently [57], can also be explained by a similar passivation model. We already showed that ethereal solvents are attacked by lithium, and the ether linkage is thus cleaved to form ROLi species [58]. We assume that PEO reacts with lithium to form elastomeric fragments of PEO with (OLi) edge groups which are, in fact, somewhat similar to those formed on lithium in DN solutions due to partial polymerization and reduction of the solvent.

Hence, we conclude that a necessary condition for stabilization of Li anodes in rechargeable battery systems is the formation of elastic, flexible surface films which can accommodate the volume changes of the anode during its electrochemical processes, thus providing it with good passivation.

3.2. Lithiated graphite electrodes

Extensive studies of lithiated graphite electrodes in a wide variety of solutions by spectroscopic means revealed that, in general, the surface chemistry of Li–C electrodes is similar to that developed on lithium and on noble metals polarized to low potentials in the same solutions [22–24]. The surface films formed on graphite electrodes during their lithiation also have a multilayer structure due to their formation process, which is usually different than that related to Li electrodes. Graphite electrodes are usually lithiated galvanostatically, which means that the surface films are formed by a highly selective process, i.e. the more reactive species which are reduced at higher potentials react first. This was indeed confirmed by a rigorous study of surface film formation on graphite at different potentials [59].

The fact that Li, Li–C and noble metals at low potentials generally develop similar surface films of relatively similar chemical structure, is reflected by impedance spectroscopy of these electrodes, as illustrated in Fig. 2. Nyquist plots obtained from these electrodes contain high frequency, flat semicircles which reflect ion transport properties and capacitance of multilayer films, which can be rigorously modeled by a 'Voight'-type analog, as was previously discussed in detail [26,27,33,38,60] and is presented in Fig. 2. The three types of electrodes shown in this figure differ in their low frequency impedance behavior.

In the case of Li metal electrodes, the Li ion migration is the rate-determining step. Other time constants related to charge transfer and Li^+ diffusion in solution phase are negligible. Thereby, the semicircle related to the surface

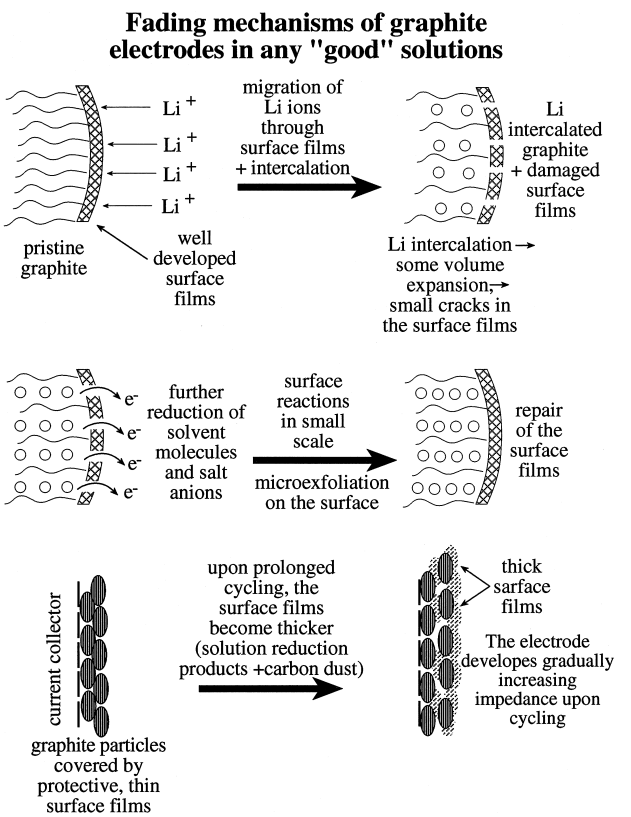

Fig. 3. A schematic illustration of surface films on graphite electrodes upon prolonged cycling.

films is the dominant feature in the spectra. Non-active metal electrodes polarized to low potentials (covered by Li ion conducting surface films) have a huge charge transfer resistance (low frequencies), which reflects the difficulty in further reduction of solution species at the low potentials when the electrode is passivated by the surface films. The impedance spectra of lithiated graphite electrodes are the most complicated because they reflect the entire Li intercalation process, which also includes, in addition to Li ion migration through the surface films and charge transfer (across the surface film–active mass interface), solid state Li ion diffusion (see the 'Warburg'-type element in Fig. 2), and accumulation of lithium in the graphite bulk. The latter stage is reflected by the lowest frequency part of the spectra, which appears as a steep Z″ vs. Z′ line from which C_{int} can be calculated according to the following formula (see discussions in Refs. [26,27]):

$$C_{int} = 1/Z'' \cdot \omega, \omega \rightarrow o \quad (15)$$

Fig. 2 also shows the various equivalent circuit analogs which relate to the different spectral features in the Nyquist plots generally obtained from lithiated graphite electrodes. Note that the charge transfer resistance, the diffusion coefficient (calculated from these spectra), and C_{int} are all potential-dependent [26,27]. Hence, the schematic spectrum in Fig. 2 represents typically stable, passivated and reversible lithiated graphite electrodes.

Stabilization of graphite electrodes is reached when reduction of solution species takes place at potentials high enough above the onset of Li intercalation (> 0.3 V vs. Li/Li^+), and lead to precipitation of passivating surface films. In contrast to lithium electrodes whose surface area and volume largely fluctuate on charge-discharge processes, the volume change of graphite during Li insertion-deinsertion is small. Thereby, precipitation of **compact** ionic species which adhere well to the graphite surface via ionic interactions are sufficient to passivate graphite electrodes, and thus lead to their highly reversible behavior [61]. Hence, when the graphite surface is covered by species such as Li_2CO_3 (formed by CO_2 reduction or by reaction of $ROCO_2Li$ species with water [25,43]), $(CH_2OCO_2Li)_2$ formed by EC reduction [25], Li_2O, SO_2, etc. [61], stable Li ion conducting and passivating surface

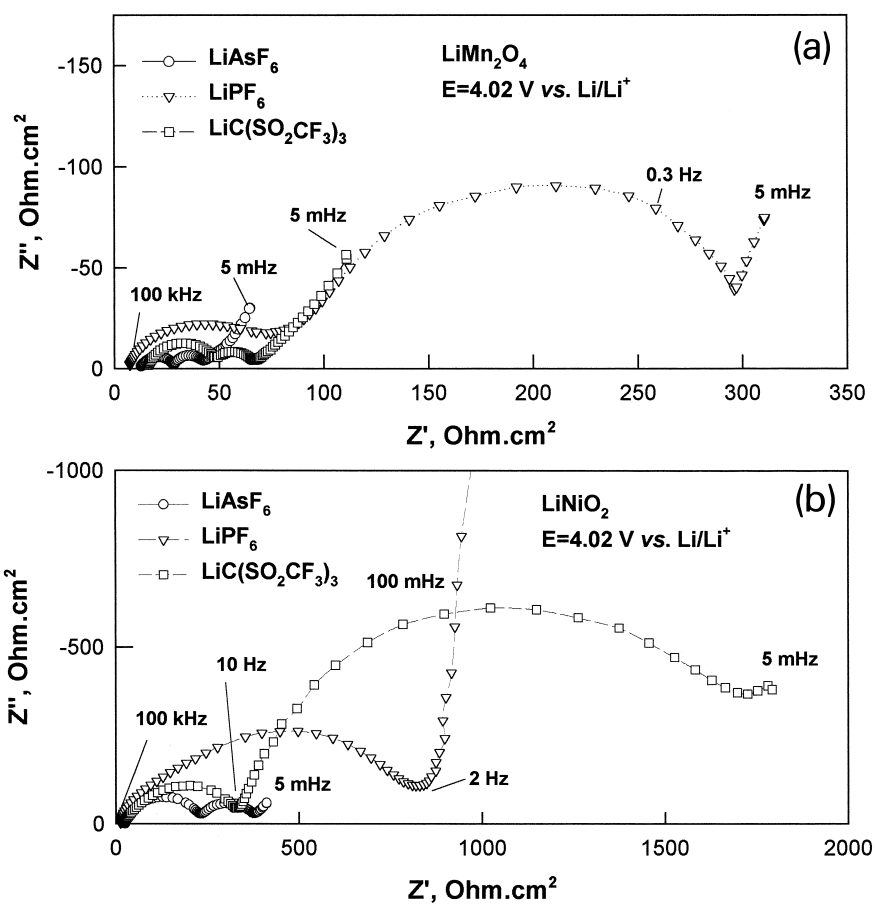

Fig. 4. Impedance spectra measured from $LiMn_2O_4$ and $LiNiO_2$ electrodes at potential around 4 V (Li/Li^+) in $LiAsF_6$, $LiPF_6$ and $LiC(SO_2CF_3)_3$ solutions in EC-DMC, as indicated. The electrodes contained ≈ 3 mg active mass per cm^2, their geometric area was around 2 cm^2, and their thickness was around 10 μm.

films are formed. Graphite electrodes have several capacity fading mechanisms, one of which involves co intercalation of solvent molecules together with Li ions (in the absence of efficient passivation), which leads to exfoliation and amorphization of the graphite [62]. This mechanism is relevant to relatively non-reactive electrolyte solutions such as ethers. Another mechanism which is relevant to propylene carbonate solution involves deactivation of the graphite particles by their electrical isolation due to surface reactions which cover the active mass by thick layers of solvent reduction products [63]. Deactivation of the graphite particles in this case is facilitated by gas bubbles (propylene) which are formed at the graphite surface, as discussed in Ref. [64]. In any event, the capacity of graphite electrodes deteriorates upon repeated charge–discharge cycling, even in optimum conditions (e.g. in solution mixtures based on EC with open chain alkyl carbonates such as DMC, DEC, EMC, etc.). This is due to an unavoidable increase in the electrode's impedance upon cycling. This situation is illustrated in Fig. 3. Due to the above-mentioned small changes in the graphite volume during Li intercalation–deintercalation, formation of cracks in the surface films which allow further reaction of the active surface with solution species on a small scale is unavoidable. This breakdown and repair of the surface films (although occurring only on a small scale), leads to a gradual thickening of the surface layer upon prolonged cycling, and hence, to an increase of the electrode's impedance.

Impedance spectroscopy of graphite electrodes during cycling in any commonly used electrolyte solution clearly indicates that the high frequency semicircle (see Fig. 2), which reflects resistance to Li ion transport through the surface films, gradually increases. Hence, in these cases, the available capacity decreases not because of destruction of the active mass, but rather due to the fact that full charging or discharging the entire active mass of the electrodes requires too high overpotentials (because of the increased electrode impedance). From the discussion above, one can conclude that very high cyclability of lithiated carbon electrodes can be obtained either by using graphite electrodes covered by surface films which contain elastomers (and thus the breakdown and repair of the surface layer can be avoided), or by shifting to carbonaceous materials of a harder structure, whose surface area and volume do not change upon Li insertion (e.g. hard, disordered carbons or graphitic carbons with some turbostratic disorder).

3.3. Li_xMO_y (M = Ni, Mn, Co, etc.)

The Li_xMO_y cathodes generally used in Li battery systems are composite electrodes in which the active mass,

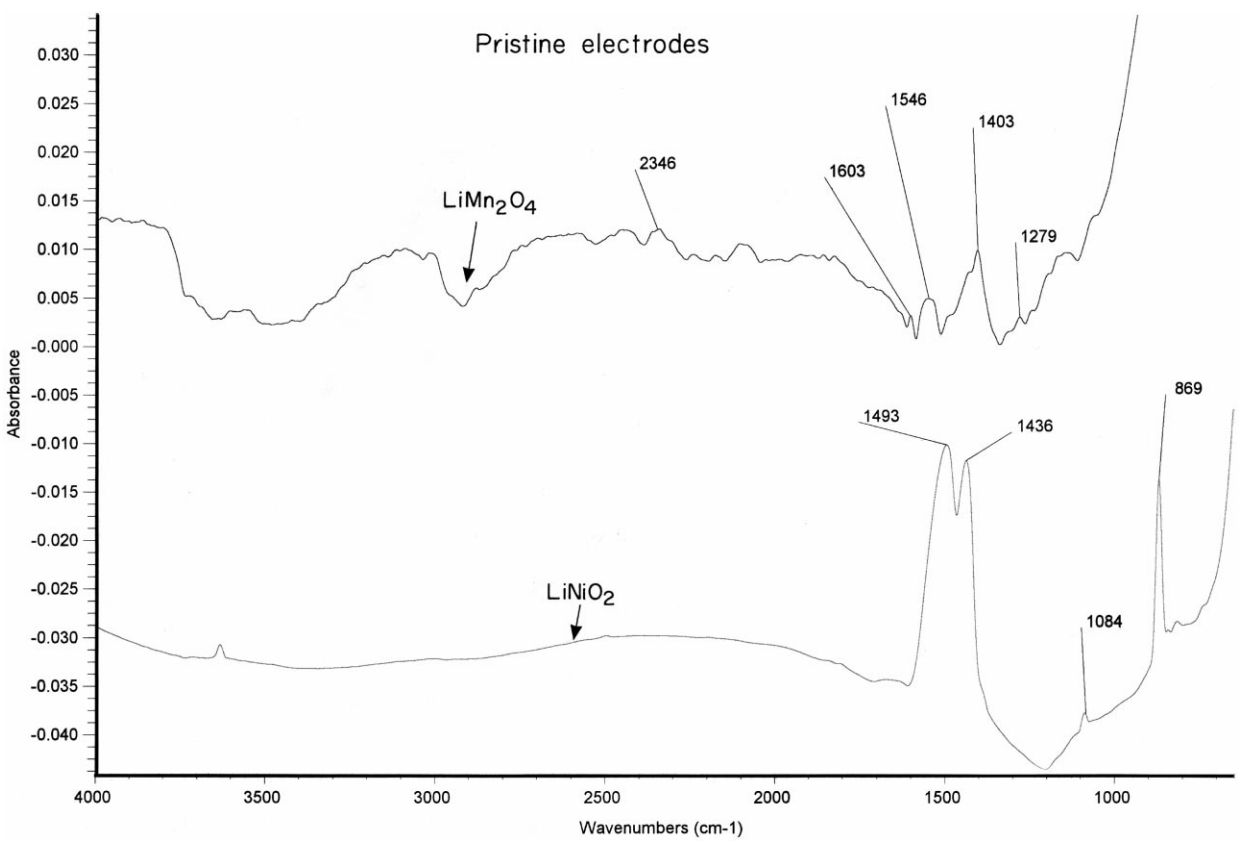

Fig. 5. FTIR spectra measured from $LiNiO_2$ and $LiMn_2O_4$ pristine powder, as indicated. Diffuse reflectance mode.

in a form of micronic particles, is mixed with a conductive additive such as carbonaceous powder, and with a polymeric binder such as PVDF, which holds the particles together and adheres them to the current collector (usually aluminum foil or grid). The electroanalytical response of such electrodes when they are thick may be too complicated to understand, because not all the particles are equally accessible to the solution, and the electrode kinetics may be highly influenced by time constants relating to ion transport in a porous structure. However, when the electrodes are thin enough (micronic thickness), prepared with an appropriate ratio between the various components, all the particles can be equally accessible to both electrons and ions and hence, the electrodes behave as an array of microelectrodes in which all the micronic particles interact simultaneously. Only in such cases is the use of fine electroanalytical tools such as EIS, PITT, GITT and SSCV [26,27] for the study of Li insertion processes really meaningful.

We discovered that many cathode materials such as $Li_xMn_2O_4$, Li_xNiO_2 and Li_xCoO_2 are covered by surface films through which Li ions have to migrate as a necessary step in the overall Li insertion process [29]. Hence, the impedance spectra of the Li_xMO_y electrodes are very similar to those obtained from the graphite electrodes, as shown schematically in Fig. 2.

Fig. 4 shows representative impedance spectra measured around 4 V (Li/Li^+) from thin $LiMn_2O_4$ (4a) and $LiNiO_2$ (4b) in EC-DMC 1:1 solutions of three salts: $LiAsF_6$, $LiPF_6$ and $LiC(SO_2CF_3)_3$, as indicated. The impedance spectra in Fig. 4 have, in general, the same elements appearing in the schematic Nyquist plot of the graphite electrode in Fig. 2: potential independent high frequency semicircle (surface films), medium-to-low frequency, potential dependent semicircle related to charge transfer, and at the low frequency the spectra contain a 'Warburg'-type element (solid state Li^+ diffusion), and then, at the very low frequency, the impedance behavior is basically capacitive and reflects the electrode's intercalation capacity as discussed above (Eq. 15). The resolution of these spectra in the low frequencies depends on the magnitude of R_{film} and R_{ct}. In cases where the electrode's resistance is too high, the above described low frequency response (i.e. a 'Warburg'-type element and capacitive behavior) can be observed only at very low frequencies (lower than 5 mHz, which is the lowest frequency that we use in EIS for practical reasons). The spectra in Fig. 4 reflect a **pronounced** difference between the two elec-

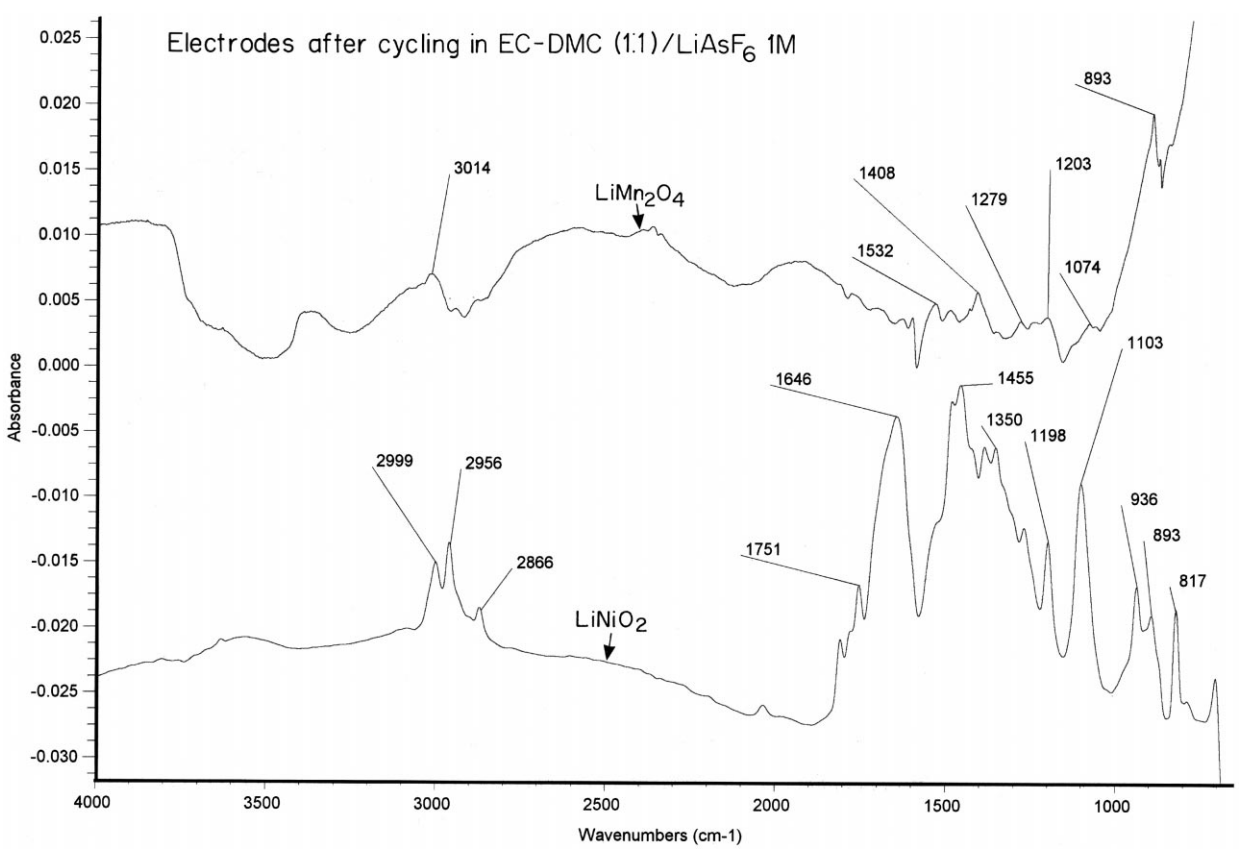

Fig. 6. FTIR spectra measured by diffuse reflectance mode from $LiNiO_2$ and $LiMn_2O_4$ electrodes (in their lithiated state) after a few charge–discharge galvanostatic cycles in EC-DMC/$LiAsF_6$ 1 M solutions.

trodes (although their structure in terms of thickness and surface area was very similar), and also the strong effect of the solution composition as summarized below:

1. In general, the impedance of the $LiNiO_2$ electrodes is much higher than that of the $LiMn_2O_4$ electrodes.
2. The impact of the salt used is also more pronounced with the $LiNiO_2$ electrodes than with the $LiMn_2O_4$ electrodes.
3. The electrode impedance is the highest in the $LiPF_6$ solution, and the lowest in the $LiAsF_6$ solution (with the impedance in $LiC(SO_2CF_3)_3$ solutions in between).

Fig. 5 shows FTIR spectra (diffuse reflectance mode, see details on the measurements in Ref. [30]) of pristine $LiMn_2O_4$ and $LiNiO_2$ electrodes (Merck), and Fig. 6 shows FTIR spectra of these electrodes after being cycled (a few charge-discharge galvanostatic cycles) in EC-DMC/$LiAsF_6$ 1 M solutions. While the spectrum of pristine $LiMn_2O_4$ only has small peaks, the spectrum of pristine $LiNiO_2$ has very pronounced Li_2CO_3 peaks. The spectra of the cycled electrodes are also quite different from each other. The spectrum of the cycled $LiNiO_2$ electrode is very rich in well-resolved IR peaks which come from organic species adsorbed on the surface. They contain strong ν_{CH} peaks around 3000–2800 cm^{-1}, $\nu_{C=O}$ (carbonyl) peaks around 1800–1600 cm^{-1}, $\delta_{CH2,CH3}$ peaks in the 1450–1300 cm^{-1} region, ν_{C-O} peaks around 1200–1100 cm^{-1} and a wealth of bending mode and ν_{C-C} stretching mode peaks below 1000 cm^{-1} (see spectral discussions in Refs. [22–25,29–31,43], etc.), In fact, the spectra from the $LiMn_2O_4$ electrode also contain many of these peaks, but at pronouncedly lower intensity and resolution. A rigorous identification of the surface compounds formed on these electrodes in these systems is beyond the scope of this publication, and is discussed in a parallel paper [65].

The source of these species may either be reflection from the anodes, i.e. $ROCO_2Li$ species formed by EC and DMC reduction on the Li or Li–C anode, and which saturate the solution, and reprecipitate on the cathode, or products of nucleophilic reactions between the oxides (negatively charged oxygen) and solvent molecules, EC and DMC, which are highly electrophilic. EDAX and XPS studies of these electrodes revealed that all three salts mentioned above also contribute to the cathode surface chemistry. $LiNiO_2$ or $LiMn_2O_4$ powder stored in their lithiated state in solutions with salts such as $LiAsF_6$, $LiPF_6$ and $LiC(SO_2CF_3)_3$ are covered by species which show fluorine peaks of LiF and insoluble moieties containing As, P or S (respectively).

These complementary studies (see discussion in Ref. [65]) proved that the above two cathode materials are intrinsically reactive with the salts and the solvents. The combination of EIS, FTIR and XPS studies of these systems clearly showed that $LiNiO_2$ is much more reactive than $LiMn_2O_4$. In addition, the high impedance of these electrodes in the $LiPF_6$ solutions is due to the massive formation of surface LiF. It is well known from the study of Li and Li–C anodes in $LiPF_6$ solutions [30] that when the surface films are comprised of LiF as a major component, they are highly resistive (two orders of magnitude more resistive than films originating from solvent reduction).

Fig. 7 compares C_{int} vs. E calculated from the EIS of $LiNiO_2$ and $LiMn_2O_4$ electrodes (Eq. 15 above), with their slow potential scan rate cyclic voltammetry (SSCV). It is important to note that C_{int} vs. E for $LiNiO_2$ at a reasonable resolution could only be calculated from data related to a $LiAsF_6$ solution, while C_{int} vs. E for $LiMn_2O_4$ could be calculated from EIS data related to the solutions of the three above salts. Fig. 7 also reflects a relatively good similarity between C_{int} vs. E and SSCV for $LiMn_2O_4$, and a much worse correlation for the $LiNiO_2$ electrodes.

Hence, it is clear that impedance spectra measured from $LiMn_2O_4$ are much better resolved than those measured from $LiNiO_2$ electrodes, because the latter electrode's surface chemistry is more intense and leads to the forma-

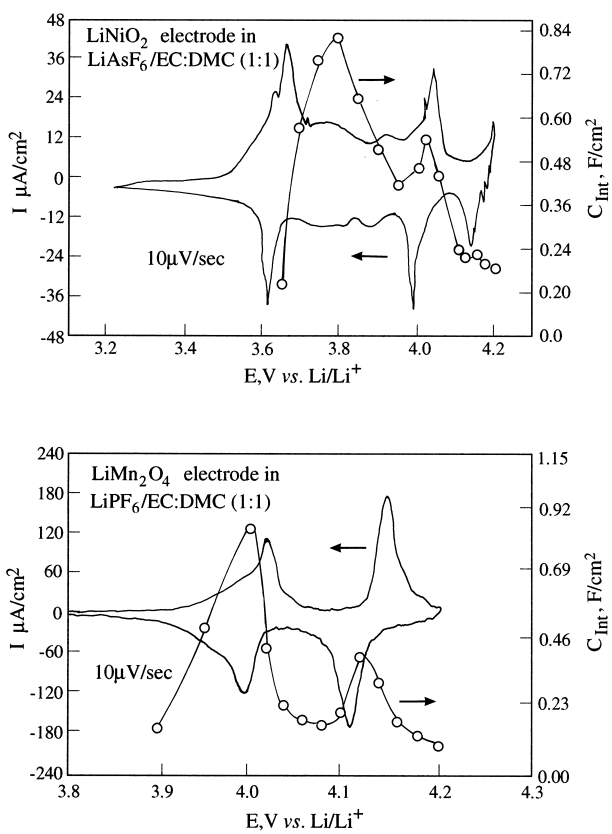

Fig. 7. C_{int} vs. E calculated from EIS data (Eq. 15, text) obtained during deintercalation of $LiNiO_2$ in EC-DMC/$LiAsF_6$ solution and $LiMn_2O_4$ in EC-DMC/$LiPF_6$ solution. These plots are compared with SSCV curves of these electrodes measured at the same solutions at 10 μV/s.

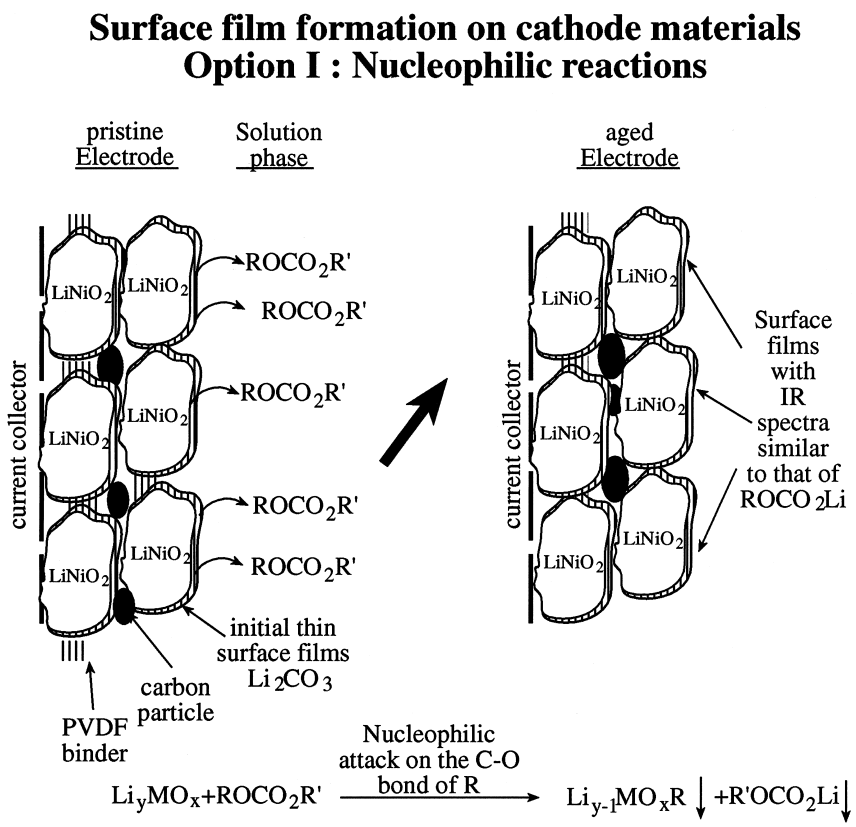

Fig. 8. Illustration of surface film formation on $LiNiO_2$ electrodes.

tion of more resistive surface films. Hence, we can distinguish here between two types of electrodes:

1. Fig. 8 illustrates the case of $LiNiO_2$ electrodes, which are very nucleophilic. The pristine electrodes are covered by Li_2CO_3 due to their reaction with CO_2 in the air. In the solutions, these pristine surface species are replaced by surface films originating from direct reactions between the active mass and the solution species.
2. Fig. 9 illustrates the cases of the $LiMn_2O_4$ spinel and Li_xMnO_2 3 V materials.

In these cases, the active mass is much less reactive with solution species than $LiNiO_2$. This allows other surface processes to take place. As discovered by Blyr et al. [66], there is a possibility of ionic exchange between $LiMn_2O_4$ and ions such as H^+ (e.g. coming from unavoidably present HF in $LiPF_6$ solutions). This leads to the formation of an inactive mass on the $LiMn_2O_4$ particles. Such phenomena lead to capacity fading of these electrodes in solutions, especially at elevated temperatures. In the case of Li_xMnO_2 electrodes (3 V), we discovered the formation of a surface $LiMn_2O_4$ spinel layer on this active mass due to interaction between this material and Li ions in solutions [67]. The formation of a spinel layer on Li_xMnO_2 leads to an anodic shift of its delithiation potential (see discussion in Ref. [67]).

4. Conclusion

The behavior of lithium, Li–C anodes and Li_xMO_y cathodes for Li batteries is strongly dependent on their surface chemistry. Stabilization of Li electrodes for rechargeable batteries may be reached only if the surface films formed on the active metal contain elastomeric, flexible components, so that the surface films can accommodate to the volume and surface changes of the Li electrodes during charge–discharge cycling. It appears that in a few limited cases such as Li electrodes in 1-3 dioxolane solutions, or in contact with PEO based electrolyte systems, this condition is fulfilled by the formation of oligomers of (CH_2–CH_2–O–) or (CH_2CH_2–OCH_2–O) (in the case of DN), which adhere to the Li surface by alkoxy (OLi) edge groups. Indeed, Li electrodes in the above two systems are exceptionally reversible.

The capacity fading mechanisms of graphite electrodes relate to the fragility of the graphite particles due to the relatively weak bonds among the graphene planes. Thereby, cointercalation of solution species can lead to graphite exfoliation. Another failure mechanism relates to aggressive surface reactions in the absence of good passivation,

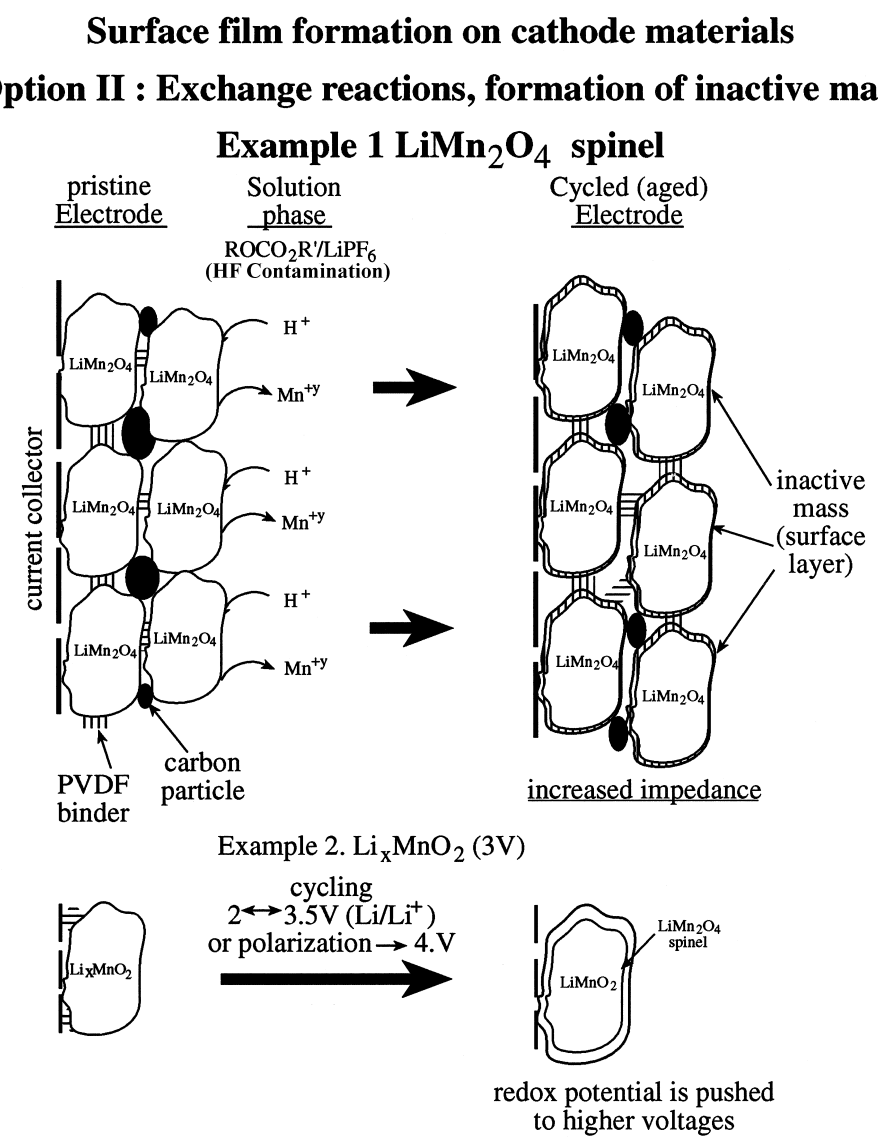

Fig. 9. Illustration of surface film formation on $LiMn_2O_4$ spinel and Li_xMnO_2 (3 V electrodes).

especially when gaseous products are formed, leading to an electrical disconnection of the active mass.

In any event, even in cases of a highly stable and reversible situation (e.g. in solutions such as EC-DMC, EC-DEC, etc.), upon prolonged charge–discharge cycling, graphite electrodes develop increasing impedance. This is because the slight volume changes in graphite during Li intercalation leads to the breakdown and repair of the surface films which thicken then.

There is an interesting similarity in the general electroanalytical behavior of Li-graphite and many Li_xMnO_y (M = Co, Ni, Mn) electrodes. This similarity is due to the fact that the cathode materials are also covered by surface films. Hence, the overall Li insertion process includes several steps in series, including Li^+ ion migration, interfacial charge transfer, solid state diffusion, etc. In the case of nucleophilic oxides such as $LiNiO_2$, there are pronounced interactions between the active mass and solution species, even in the lithiated state. This leads to massive surface film precipitation. Other cathode materials such as $LiMn_2O_4$ spinel and Li_xMnO_2 (3 V materials) are less nucleophilic, and thereby, their surface reactions with solvent molecules or salt anions are not pronounced. This opens the door for other classes of interactions such as ionic exchange, which also leads to the formation of surface layers. However, in these cases, these layers are not comprised of organic or inorganic Li salts, but rather contain mostly modified Li_xMnO_y species.

Acknowledgements

Partial support for this work was obtained from Merck, Germany, NEDO — New Energy Development Organization, Japan, the Israeli National Science Foundation (NSF), and the German Ministry of Science BMBF, within the framework of the DIP program.

References

[1] P. Novak, K. Muller, K.S.V. Santhanam, O. Hass, Chem. Rev. 97 (1997) 207.
[2] M. Liu, S.J. Visco, L.C. De Jonghe, J. Electrochem. Soc. 138 (1996) 1896.
[3] T. Ohzuku, in: G. Pistoia (Ed.), Li batteries, new materials, developments and perspectives, Elsevier, Amsterdam, 1994, pp. 239–280, Chap. 6.
[4] P. Dan, E. Mengeritsky, Y. Geronov, D. Aurbach, I. Weissman, J. Power Sources 54 (1995) 143.
[5] B. Scrosati, Nature 373 (1995) 557.
[6] S. Hossain, in: D. Linden (Ed.), Handbook of Batteries, 2nd edn., McGraw-Hill, New York, 1995, Chap. 36.
[7] L. Dominey, in: D. Aurbach (Ed.), Non-aqueous Electrochemistry, Marcel Dekker, New York, 1999, Chap. 8.
[8] M. Wakihara, O. Yamamoto, Li ion Batteries, Fundamental and Performance, Wiley, Weinheim, NY, 1998, and references therein.
[9] A.R. Armstrong, A.D. Robertson, R.L. Gitzendanner, P.G. Bruce, J. Chem. Soc., Chem. Commun. (1998) 1833.
[10] H. Kawai, M. Nagata, H. Takamoto, A.R. West, J. Mater. Chem. 10 (1998) 3266.
[11] G.T.-K. Fey, W. Li, J.R. Dahn, J. Electrochem. Soc. 141 (1994) 2279.
[12] E. Buiel, A.E. George, J.R. Dahn, J. Electrochem. Soc. 145 (1998) 1977.
[13] G.G. Amatucci, C.N. Schmutz, A. Blyr, C. Sigala, A.S. Gozdz, D. Larcher, J.-M. Tarascon, J. Power Sources 69 (1997) 11.
[14] G. Ceder, Y.-M. Chiang, D.R. Sadoway, M.K. Aydinol, Y.-L. Jang, B. Huang, Nature 392 (1998) 694.
[15] T. Ohzuku, in: J.O. Besenhard (Ed.), Handbook of Battery Materials, Wiley-VCH, Weinheim, New York, Singapore, Toronto, 1998.
[16] J. Teslic, T. Egami, J.E. Fischer, Phys. Rev. B 15 (1995) 5973.
[17] M. Inaba, Z. Siroma, A. Funobiki, Z. Ogumi, T. Abe, Y. Mizutani, M. Asano, Langmuir 12 (1996) 1535.
[18] C. Menachem, Y. Wang, J. Flowers, E. Peled, S.G. Greenbaum, J. Power Sources 76 (1998) 180.
[19] D.S. Ginley, J.D. Perkins, J.M. McGraw, P.A. Parilla, M.L. Fu, C.T. Rogers, Mat. Res. Soc. Symp. Proc., 496 (1998) 293–302, 373–378.
[20] M. Watanabe, A. Nishimoto, Solid State Ionics 79 (1995) 306.
[21] P. Novak, W. Scheifele, F. Joho, O. Haas, J. Electrochem. Soc. 142 (1995) 2544.
[22] D. Aurbach, A. Zaban, Y. Gofer, Y. Ein-Eli, I. Weissman, O. Chusid, O. Abramson, B. Markovsky, J. Power Sources 54 (1995) 76.
[23] D. Aurbach, A. Zaban, Y. Ein-Eli, I. Weissman, O. Chusid, B. Markovsky, M.D. Levi, E. Levi, A. Schechter, E. Granot, J. Power Sources 86 (1997) 91.
[24] D. Aurbach, B. Markovsky, M.D. Levi, A. El Levi, M. Schechter, Y. Moshkovich, J. Power Sources (1999) in press.
[25] D. Aurbach, Y. Ein-Eli, A. Zaban, J. Electrochem. Soc. 141 (1994) L1.
[26] M. D. Levi, D. Aurbach, J. Electroanal. Chem., 421 (1997) 79, 89.
[27] D. Aurbach, M.D. Levi, J. Phys. Chem. B, 101 (1997) 4630, 4641.
[28] Z. Lu, A. Schechter, M. Moshkovich, D. Aurbach, J. Electroanal. Chem. 466 (1999) 203.
[29] D. Aurbach, M.D. Levi, E. Levi, H. Teller, B. Markovsky, G. Salitra, L. Heider, U. Heider, J. Electrochem. Soc. 145 (1998) 3024.
[30] D. Aurbach, B. Markovsky, A. Schechter, Y. Ein-Eli, H. Cohen, J. Electrochem. Soc. 143 (1996) 3809.
[31] D. Aurbach, O. Chusid, I. Weissman, Electrochim. Acta 41 (1996) 747.
[32] A. Zaban, D. Aurbach, J. Electroanal. Chem. 348 (1993) 155.
[33] D. Aurbach, A. Zaban, J. Electroanal. Chem. 367 (1994) 15.
[34] D. Aurbach, Y. Ein-Eli, J. Electrochem. Soc. 142 (1995) 1746.
[35] D. Aurbach, E. Levi, M.D. Levi, R. Oesten, U. Heider, L. Heider, J. Solid State Ionics (1999) in press.
[36] D. Aurbach, Y. Cohen, J. Electrochem. Soc. 143 (1996) 3525.
[37] D. Aurbach, M. Moshkovich, J. Electrochem. Soc. 145 (1998) 2629.
[38] D. Aurbach, A. Zaban, J. Electrochem. Soc. 141 (1994) 1808.
[39] D. Aurbach, I. Weissman, A. Zaban, Y. Ein-Eli, E. Mengeritsky, P. Dan, J. Electrochem. Soc. 143 (1996) 2110.
[40] P. Dan, E. Mengeritsky, I. Weissman, E. Zinigrad, J. Power Sources 68 (1997) 443.
[41] D. Aurbach, I. Weissman, A. Schechter, H. Cohen, Langmuir 12 (1996) 3991.
[42] A. Schechter, D. Aurbach, Langmuir 15 (1999) 3334.
[43] D. Aurbach, H.E. Gottlieb, Electrochim. Acta 34 (1989) 141.
[44] D. Aurbach, Y. Ein-Eli, Langmuir 8 (1992) 1845.
[45] K. Kanamura, H. Tamura, S. Shiraishi, Z.-I. Takehara, Electrochim. Acta 40 (1995) 913.
[46] K. Kanamura, H. Tamura, Z.-I. Takehara, J. Electroanal. Chem. 333 (1992) 127.
[47] K. Kanamura, H. Tamura, S. Shiraishi, Z.-I. Takehara, J. Electroanal. Chem. 394 (1995) 49.
[48] T. Fujieda, N. Yamamoto, K. Saito, T. Ishibashi, M. Honjo, S. Koike, N. Wakabayashi, S. Higuchi, J. Power Sources 52 (1994) 197.
[49] K. Kanamura, H. Takezawa, S. Shiraishi, Z. Takehara, J. Electrochem. Soc. 144 (1997) 1900.
[50] D. Aurbach, J. Electrochem. Soc. 136 (1989) 1610.
[51] M. Odziemkowski, D.E. Irish, J. Electrochem. Soc. 193 (1992) 3063.
[52] G. Zhuang, P.N. Ross, F.P. Kong, F. McLarnon, J. Electrochem. Soc. 145 (1998) 159.
[53] E. Peled, in: J.P. Gabano (Ed.), Li Batteries, Academic Press, London, 1983, Chap. 3.
[54] D. Aurbach, Y. Gofer, M. Ben-Zion, J. Power Sources 39 (1992) 163.
[55] O. Youngman, Y. Gofer, A. Meitav, D. Aurbach, Electrochim. Acta 35 (1990) 625.
[56] D. Aurbach, I. Weissman, H. Yamin, E. Elster, J. Electrochem. Soc. 145 (1998) 1421.
[57] M. Gauthier, Presentation of the work at Hydro Quebec (Canada) on Li polymer batteries at several recent international meetings, private communication.
[58] D. Aurbach, E. Granot, Electrochim. Acta 42 (1997) 697.
[59] S. Mori, H. Asahina, H. Suzuki, A. Yonei, K. Yokoto, J. Power Sources 68 (1997) 59.
[60] D. Aurbach, A. Zaban, J. Power Sources 54 (1995) 289.
[61] Y. Ein-Eli, Electrochem. Solid State Lett. 2 (1999) 212.
[62] M. Winter, J.O. Besenhard, M.E. Spahr, P. Novak, Adv. Mater. 10 (1998) 725.
[63] D. Aurbach, M.D. Levi, E. Levi, A. Schechter, J. Phys. Chem. B 101 (1997) 2195.
[64] D. Aurbach, B. Markovsky, I. Weissman, E. Levi, Y. Ein-Eli, Electrochim. Acta 45 (1999) 167.
[65] D. Aurbach, K. Gamolsky, B. Markovsky, G. Salitra, Y. Gofer, J. Electrochem. Soc. (2000) in press.
[66] A. Blyr, C. Sigala, G.G. Amatucci, D. Guyomard, Y. Chabra, J.-M. Tarascon, J. Electrochem. Soc. 145 (1998) 194.
[67] E. Mengeritsky, E. Elster, E. Granot, P. Dan, H. Yamin, E. Levi, E. Zinigrad, H. Teller, M.D. Levi, D. Aurbach, J. Electrochem. Soc. 144 (1997) 4133.